# Supplementary Information

## Fire/Heat-Resistant, Anti-Corrosion and Folding $Ti_2C_3T_x$ MXene/Single-Walled Carbon Nanotube Film for Extreme-Environmental EMI Shielding and Solar-thermal Conversion Applications

Bing Zhou,[a] Yanli Li,[a] Zhaoyang Li,[a,b*] Jianmin Ma,[c] Keqing Zhou,[d] Chuntai Liu,[a] Changyu Shen[a], Yuezhan Feng[a*]

[a]*Key Laboratory of Materials Processing and Mold Ministry of Education, National Engineering Research Center for Advanced Polymer Processing Technology, Zhengzhou University, Zhengzhou 450002, China.*

[b]*Shangqiu Normal University, Shangqiu 476000, China.*

[c]*Key Laboratory for Micro-/Nano-Optoelectronic Devices, Ministry of Education, School of Physics and Electronics, Hunan University, Changsha 410022, China.*

[d]*Faculty of Engineering, China University of Geosciences (Wuhan), Wuhan 430074, China.*

*Corresponding Authors, E-mail: lizhaoyang@sqnu.edu.cn (Z. Li) and yzfeng@zzu.edu.cn (Y. Feng).

### Experimental Section

***Preparation of MXene nanosheets.*** LiF (2 g) was dissolved in 40 mL HCl solution (9 M), and then $Ti_3AlC_2$ powers (2 g) were added and magnetically stirred at 35 °C for 24 h. Subsequently, the resulting suspension was purified with DI water through repeated dispersion and centrifugation until the pH value of solution was close to 7. Afterwards,

the sediment was dispersed in ethanol and ultrasonicated for 60 min. The suspension was centrifuged again for 3 min under 3500 rpm to remove the unexfoliated $Ti_3AlC_2$. Finally, a colloidal suspension containing single- and/or few-layered MXene nanosheets was achieved.

***Dispersion of CNT:*** SWNT solution was achieved by dispersing the SWNTs and SDS (mass ratio 1:5) in deionized water. The SWNTs and SDS were mixed and sonicated in a bath sonicator at 100 W for 0.5 h and followed in probe sonicator at 325 W for 1 h.

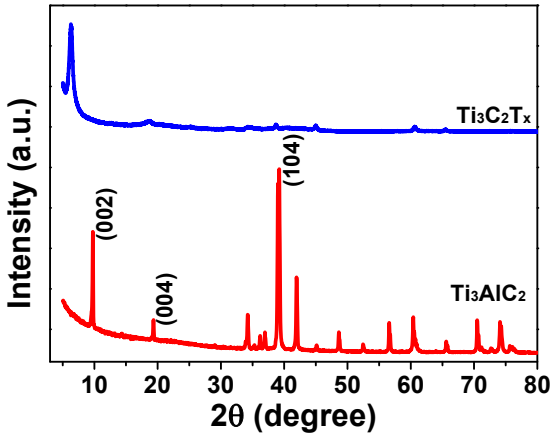


**Figure S1.** XRD patterns of $Ti_3C_2T_x$ MXene and $Ti_3AlC_2$ MAX phase.

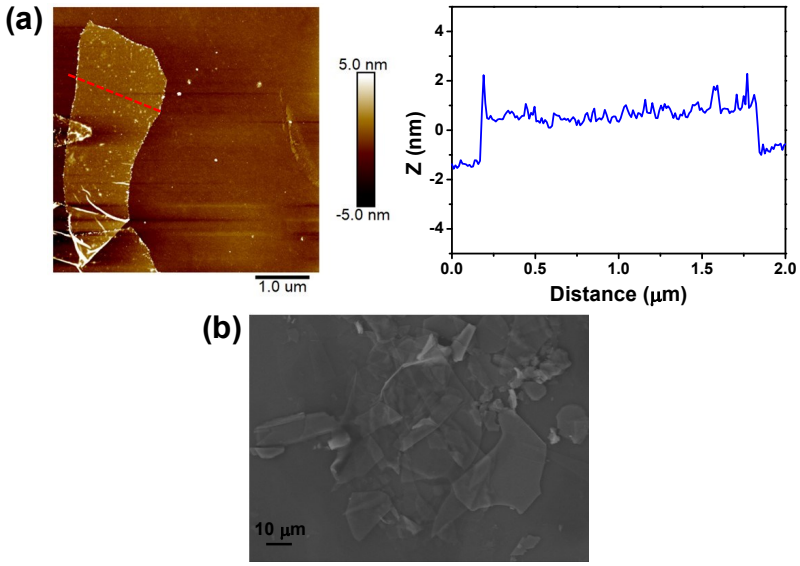

**Figure S2.** (a) AFM and (b) SEM of $Ti_3C_2T_x$ MXene.

**Figure S3.** Photographs of SWNTs suspension.

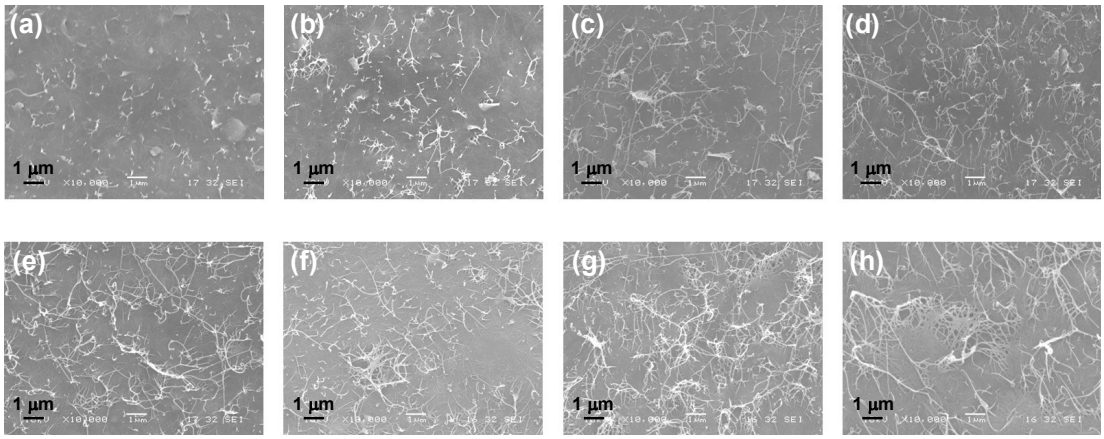


**Figure S4.** SEM images of surface of (a) MXene/$CNT_{9:1}$, (b) MXene/$CNT_{8:2}$, (c) MXene/$CNT_{7:3}$, (d) MXene/$CNT_{6:4}$, (e) MXene/$CNT_{4:6}$, (f) MXene/$CNT_{3:7}$, (g) MXene/$CNT_{2:8}$, and (h) MXene/$CNT_{1:9}$ films.

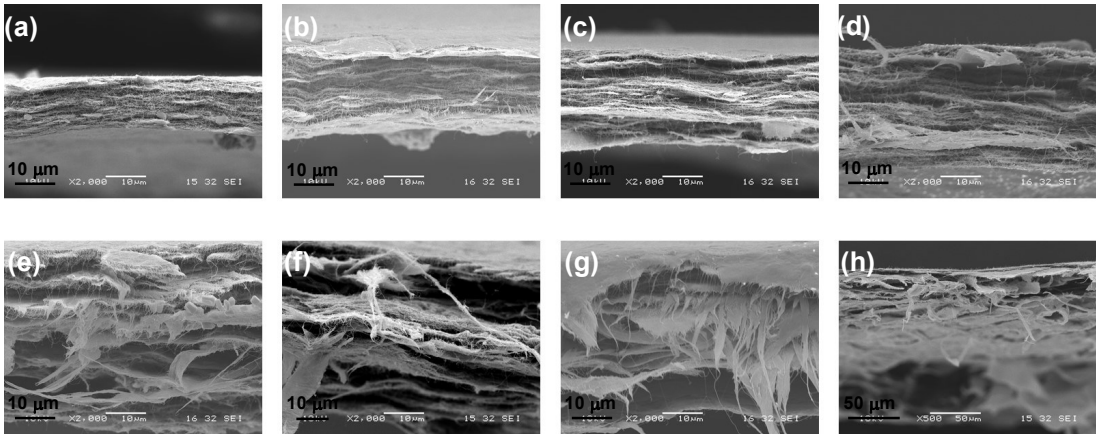


**Figure S5.** SEM images of cross-section of (a) MXene/$CNT_{9:1}$, (b) MXene/$CNT_{8:2}$, (c) MXene/$CNT_{7:3}$, (d) MXene/$CNT_{6:4}$, (e) MXene/$CNT_{4:6}$, (f) MXene/$CNT_{3:7}$, (g) MXene/$CNT_{2:8}$, and (h) MXene/$CNT_{1:9}$ films.

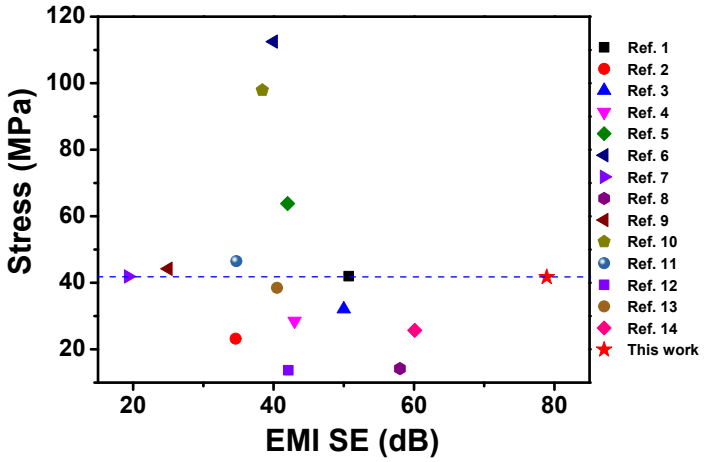


**Figure S6.** Comparison of stress and average EMI SE in X-band.

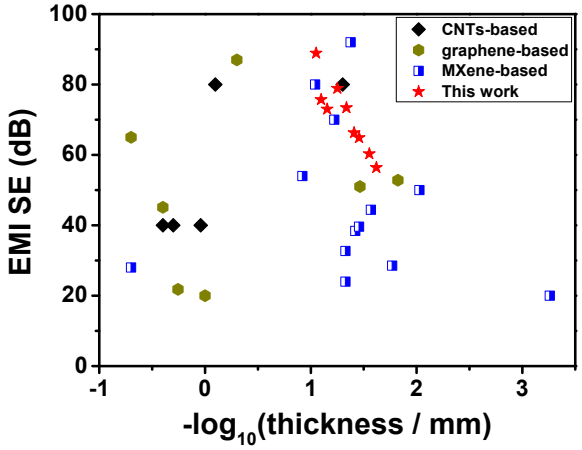

**Figure S7.** Shielding performance comparison.

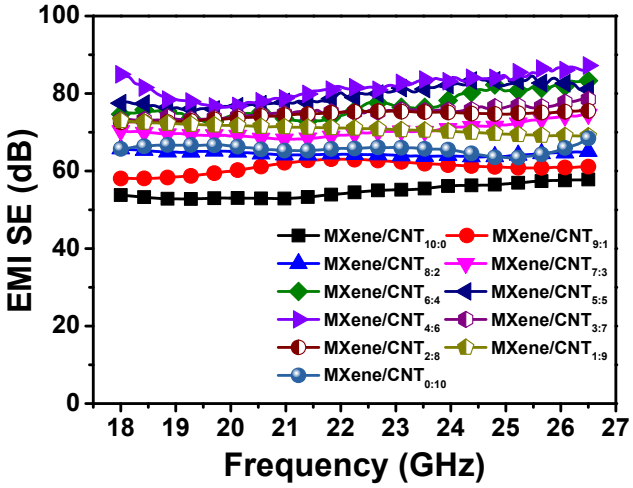


**Figure S8.** EMI shielding performance in K-band.

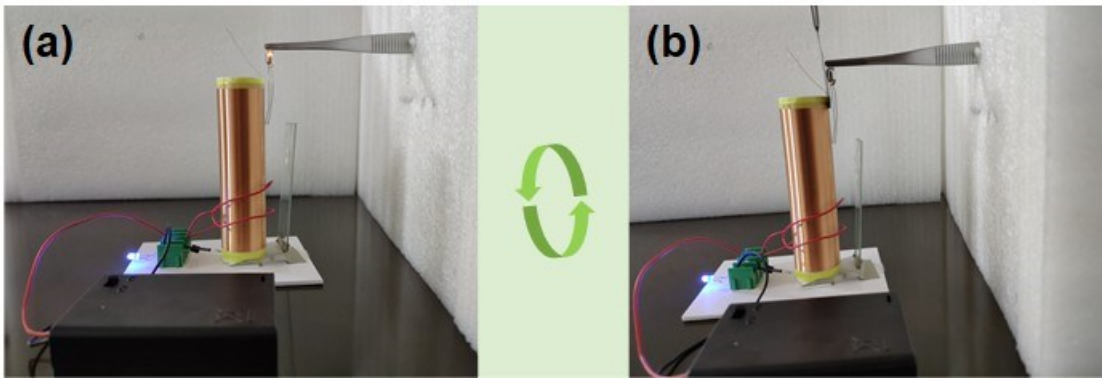


**Figure S9.** Photographs of wireless power-transfer circuit (a) without and (b) with the prepared MXene/CNTs film, where the induced LED can be turned off by the shielding effect of as-prepared MXene/CNTs film.

Figure S9 show a typical wireless power transmission system consisting of a DC power, transistors, transmitter coil, receiver coil, and light-emitting diode (LED) lights. When the circuit is switched on, the direct current is converted to alternating current with the help of a transistor, creating an electromagnetic field. Subsequently, the LED is turned

on due to the electromotive force generated in the receiver coil by the electromagnetic induction (Figure S9a). When MXene/CNT film is inserted between the two coils, the LED light is turned off, because the electromagnetic transmission is blocked (Figure S9b and Movie S1). This simple experiment further proves that MXene/CNTs film has excellent EMI shielding performance.

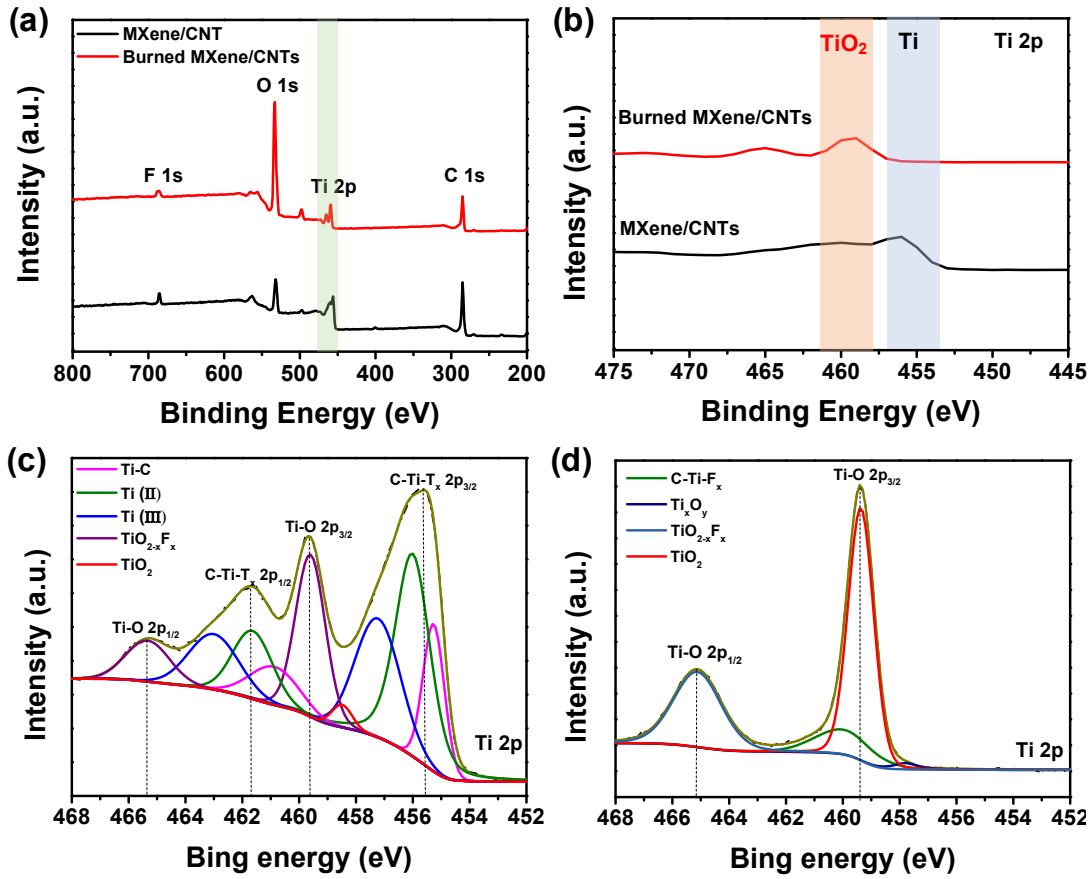


**Figure S10.** (a) XPS spectra and (b) their enlarged view of MXene/CNT film before and after burning. High-resolution XPS spectra at Ti 2p for (c) MXene/CNT film and (d) burned MXene/CNT film.

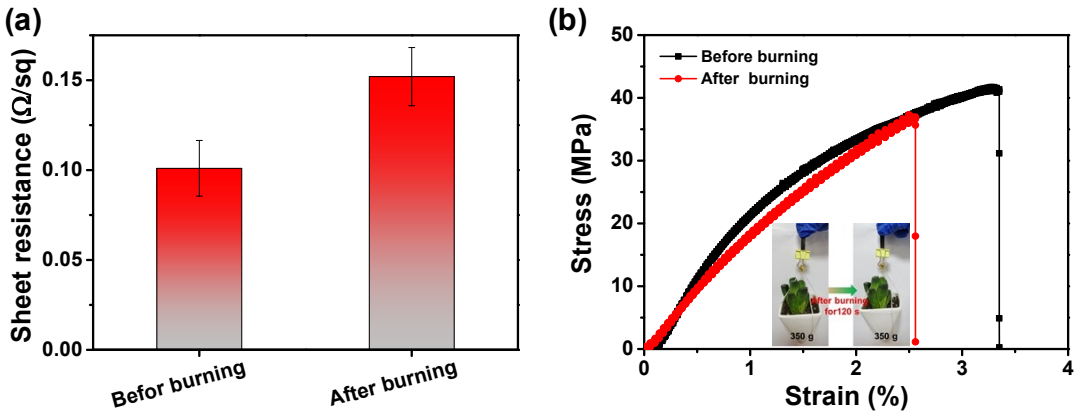


**Figure S11.** (a) Sheet resistance and (b) tensile stress−strain curves of MXene/$CNT_{4:6}$ film before and after burning. **Inset:** Digital images of MXene/$CNT_{4:6}$ film ithstanding a pot flower before and after burning treatment.

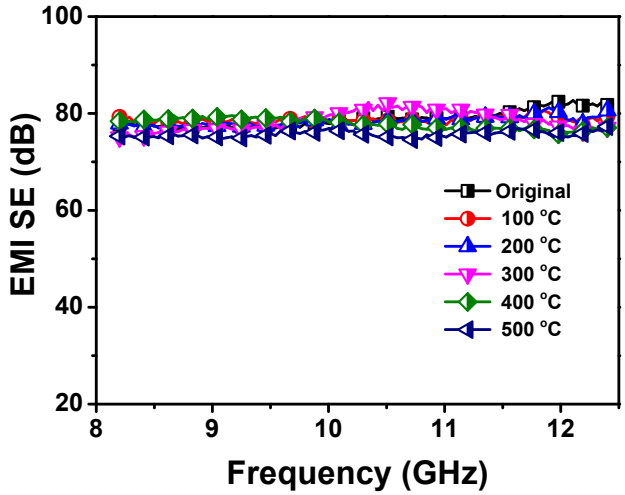


**Figure S12.** EMI shielding performance of MXene/$CNT_{4:6}$ film at different temperatures.

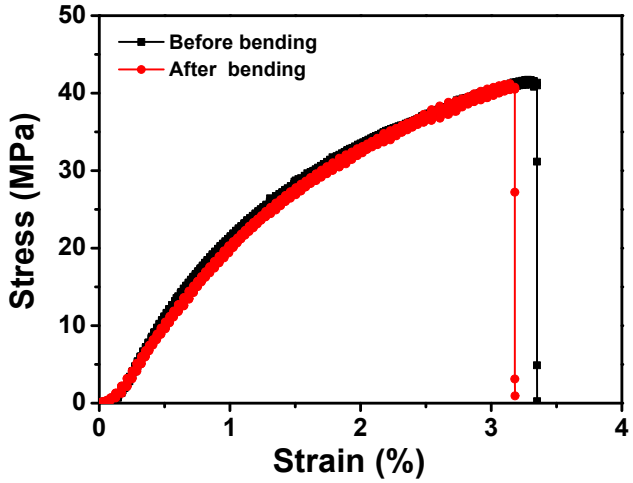


**Figure S13.** Tensile stress−strain curves of MXene/$CNT_{4:6}$ film before and after bending for 1000 times.

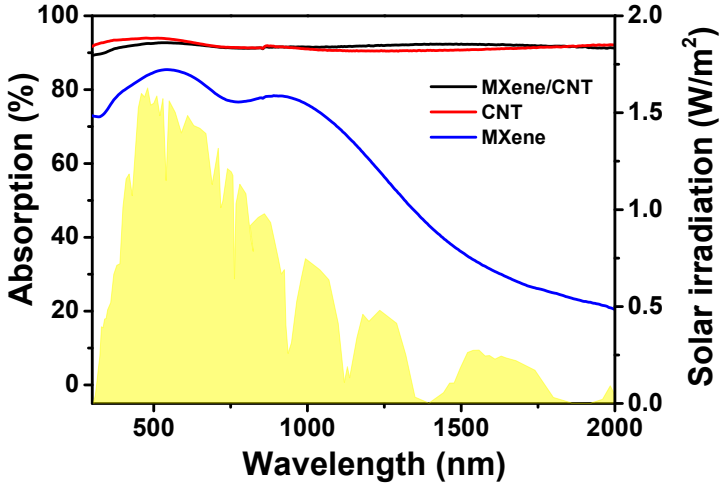


**Figure S14.** UV–vis–NIR absorption spectra of pure MXene, pure CNT, MXene/$CNT_{4:6}$ films.

**Table S1.** Comprehensive comparison in view of conductivity, mechanical strength and EMI shielding performance with previous literatures.

| Sample | Conductiv (S/cm) | EMI SE (dB) | Tensile strength (MPa) | Ref. |
|---|---|---|---|---|
| MXene/TPU | 16 | 50.7 | 42 | [1] |
| MXene/FG | 8.97 | 34.6 | 23.2 | [2] |

| | | | | |
|---|---|---|---|---|
| MXene/CNF/Ag | 5.88 | 50 | 32.1 | [3] |
| MXene/NR | 293.3 | 43 | 28.5 | [4] |
| MXene/AgNW/NC | 300 | 42 | 63.8 | [5] |
| MXene/TOCNF | 621 | 40 | 112.5 | [6] |
| MXene/Ni chain/PVDF | 892 | 19.3 | 41.9 | [7] |
| $Fe_3O_4$@$Ti_3C_2T_x$/ENR | - | 58 | 14.2 | [8] |
| MXene/CNF | 739.4 | 25 | 44.2 | [9] |
| MXene/CNTs/CNF | 2506.6 | 38.4 | 97.9 | [10] |
| MXene/ANF | - | 34.7 | 46.5 | [11] |
| MXene/PEDOT:PSS | 340.5 | 42.1 | 13.7 | [12] |
| MXene/PEDOT:PSS | - | 40.5 | 38.5 | [13] |
| MXene/Cellulose | 59.4 | 60.1 | 25.7 | [14] |
| MXene/$CNTs_{4:6}$ | 1854.9 | 78.9 | 41.7 | This work |

**Table S2.** Comparison of EMI SSE versus thickness of MXene/CNTs film and other materials.

| Category | Samples | Thickness (mm) | EMI SE (dB) | Ref. |
|---|---|---|---|---|
| CNTs-based | SWCNT/Graphene | 0.05 | 80 | [15] |
| | MWCNT/Epoxy | 2 | 40 | [16] |
| | Carbon/Cellulose | 2.5 | 40 | [17] |
| | MWCNT/WPU | 0.8 | 80 | [18] |
| | MWCNT/ABS | 1.1 | 40 | [19] |

| | | | | |
|---|---|---|---|---|
| Graphene-based | rGO/CNT/Co/C | 0.0343 | 51 | [20] |
| | rGO /TPU | 1.8 | 21.8 | [21] |
| | graphene/PDMS | 5 | 65 | [22] |
| | rGO@Fe3O4/T-ZnO/Ag/WPU | 0.5 | 87 | [23] |
| | rGO /PS | 2.5 | 45.1 | [24] |
| | Graphene/PDMS | 1 | 20 | [25] |
| | rGO /CNT | 0.015 | 52.8 | [26] |
| MXene-based | d-$Ti_3C_2T_x$/ANF | 0.017 | 28.54 | [27] |
| | $Ti_3C_2T_x$/TOCNF-50 | 0.047 | 32.7 | [28] |
| | $Ti_3C_2T_x$/CNF | 0.047 | 24 | [9] |
| | $Ti_3C_2T_x$/PVA | 5 | 28 | [29] |
| | CNT/MXene/CNF | 0.038 | 38.4 | [10] |
| | PVA/MXene | 0.027 | 44.4 | [30] |
| | CNF5@MXene4 | 0.035 | 39.6 | [31] |
| | $Ti_3C_2T_x$ film | 0.0094 | 50 | [32] |
| | $Ti_3C_2T_x$ film | 0.00055 | 20 | [33] |
| | ANF-MXene/AgNW | 0.091 | 80 | [34] |
| | MXene/AgNW Silk Textiles | 0.12 | 54 | [35] |
| | MXene foam | 0.06 | 70 | [36] |
| | $Ti_3C_2T_x$ film | 0.042 | 92 | [37] |
| | $MXene/CNTs_{10:0}$ | 0.018 | 50.3 | This Work |
| | $MXene/CNTs_{9:1}$ | 0.024 | 56.4 | |

| | | | |
|---|---|---|---|
| | MXene/CNTs$_{8:2}$ | 0.028 | 60.3 |
| | MXene/CNTs$_{7:3}$ | 0.035 | 64.9 |
| | MXene/CNTs$_{6:4}$ | 0.039 | 66.3 |
| | MXene/CNTs$_{5:5}$ | 0.046 | 73.4 |
| | MXene/CNTs$_{4:6}$ | 0.056 | 78.9 |
| | MXene/CNTs$_{3:7}$ | 0.070 | 73.0 |
| | MXene/CNTs$_{2:8}$ | 0.08 | 75.7 |
| | MXene/CNTs$_{1:9}$ | 0.089 | 88.9 |
| | MXene/CNTs$_{0:10}$ | 0.092 | 52.4 |

**Supporting Movie 1.** Burning process of the MXene/CNTs film.

**Supporting Movie 2.** Burning process of the MXene/CNTs film connected to a white LED lamp as a conducting wire.

**Supporting Movie 3.** EMI shielding behavior of MXene/CNTs film, showing the film efficiently shields EM waves.

## References


1. Q. Gao, Y. Pan, G. Zheng, C. Liu, C. Shen and X. Liu, *Adv. Compos. Hybrid Mater.*, 2021, DOI: 10.1007/s42114-021-00221-4.
2. X. Jia, B. Shen, L. Zhang and W. Zheng, *Compos. Part B-Eng.*, 2020, **198**,108250.
3. W. Xin, G.-Q. Xi, W.-T. Cao, C. Ma, T. Liu, M.-G. Ma and J. Bian, *RSC Adv.*,

2019, **9**, 29636-29644.

4. Y. Wang, R. Liu, J. Zhang, M. Miao and X. Feng, *Appl. Surf. Sci.*, 2021, **546**,149143.

5. M. Miao, R. Liu, S. Thaiboonrod, L. Shi, S. Cao, J. Zhang, J. Fang and X. Feng, *J. Mater. Chem. C*, 2020, **8**, 3120-3126.

6. B. Zhou, Z. Zhang, Y. Li, G. Han, Y. Feng, B. Wang, D. Zhang, J. Ma and C. Liu, *ACS Appl. Mater. Interfaces*, 2020, **12**, 4895-4905.

7. S. J. Wang, D. S. Li and L. Jiang, *Adv. Mater. Interfaces*, 2019, **6**, 1900961.

8. Q. Song, B. Chen, Z. Zhou and C. Lu, *Sci. China Mater.*, 2021, DOI: 10.1007/s40843-020-1539-2.

9. W. T. Cao, F. F. Chen, Y. J. Zhu, Y. G. Zhang, Y. Y. Jiang, M. G. Ma and F. Chen, *ACS Nano*, 2018, **12**, 4583-4593.

10. W. Cao, C. Ma, S. Tan, M. Ma, P. Wan and F. Chen, *Nano-Micro Lett.*, 2019, **11**, 2-17.

11. H. Wei, M. Wang, W. Zheng, Z. Jiang and Y. Huang, *Ceram. Int.*, 2020, **46**, 6199-6204.

12. R. Liu, M. Miao, Y. Li, J. Zhang, S. Cao and X. Feng, *ACS Appl. Mater. Interfaces*, 2018, **10**, 44787-44795.

13. Y.-J. Wan, X.-M. Li, P.-L. Zhu, R. Sun, C.-P. Wong and W.-H. Liao, *Compos. Part A-Appl. S.*, 2020, **130**,105764.

14. M. Zhu, X. Yan, H. Xu, Y. Xu and L. Kong, *Ceram. Int.*, 2021, DOI: 10.1016/j.ceramint.2021.03.034.

15. H. Fu, Z. Yang, Y. Zhang, M. Zhu, Y. Jia, Z. Chao, D. Hu and Q. Li, *Carbon*, 2020, **162**, 490-496.

16. Y. Chen, H.-B. Zhang, Y. Yang, M. Wang, A. Cao and Z.-Z. Yu, *Adv. Funct. Mater.*, 2016, **26**, 447-455.

17. L. Q. Zhang, S. G. Yang, L. Li, B. Yang, H. D. Huang, D. X. Yan, G. J. Zhong, L. Xu and Z. M. Li, *ACS Appl. Mater. Interfaces*, 2018, **10**, 40156-40167.

18. Z. Zeng, M. Chen, H. Jin, W. Li, X. Xue, L. Zhou, Y. Pei, H. Zhang and Z. Zhang, *Carbon*, 2016, **96**, 768-777.

19. M. H. Al-Saleh, W. H. Saadeh and U. Sundararaj, *Carbon*, 2013, **60**, 146-156.

20. M. Yang, Q. Wei, J. Li, Y. Wang, H. Guo, L. Gao, L. Huang, X. He, Y. Li and Y. Yuan, *Adv. Mater. Interfaces*, 2020, **7**, 1901815.

21. Q. Jiang, X. Liao, J. Li, J. Chen, G. Wang, J. Yi, Q. Yang and G. Li, *Compos. Part A-Appl. S.*, 2019, **123**, 310-319.

22. W. Gao, N. Zhao, T. Yu, J. Xi, A. Mao, M. Yuan, H. Bai and C. Gao, *Carbon*, 2020, **157**, 570-577.

23. Y. Xu, Y. Yang, D. X. Yan, H. Duan, G. Zhao and Y. Liu, *ACS Appl. Mater. Interfaces*, 2018, **10**, 19143-19152.

24. D.-X. Yan, H. Pang, B. Li, R. Vajtai, L. Xu, P. G. Ren, J. H. Wang and Z. M. Li, *Adv. Funct. Mater.*, 2015, **25**, 559-566.

25. Z. Chen, C. Xu, C. Ma, W. Ren and H. M. Cheng, *Adv. Mater.*, 2013, **25**, 1296-1300.

26. E. Zhou, J. Xi, Y. Guo, Y. Liu, Z. Xu, L. Peng, W. Gao, J. Ying, Z. Chen and C.

Gao, *Carbon*, 2018, **133**, 316-322.

27. F. Xie, F. Jia, L. Zhuo, Z. Lu, L. Si, J. Huang, M. Zhang and Q. Ma, *Nanoscale*, 2019, **11**, 23382-23391.

28. Z. Zhan, Q. Song, Z. Zhou and C. Lu, *J. Mater. Chem. C*, 2019, **7**, 9820-9829.

29. H. Xu, X. Yin, X. Li, M. Li, S. Liang, L. Zhang and L. Cheng, *ACS Appl. Mater. Interfaces*, 2019, **11**, 10198-10207.

30. X. Jin, J. Wang, L. Dai, X. Liu, L. Li, Y. Yang, Y. Cao, W. Wang, H. Wu and S. Guo, *Chem. Eng. J.*, 2020, **380**, 122475.

31. B. Zhou, Z. Zhang, Y. Li, G. Han, Y. Feng, B. Wang, D. Zhang, J. Ma and C. Liu, ACS Appl. Mater. Interfaces, 2020, **12**, 4895-4905.

32. J. Zhang, N. Kong, S. Uzun, A. Levitt, S. Seyedin, P. A. Lynch, S. Qin, M. Han, W. Yang, J. Liu, X. Wang, Y. Gogotsi and J. M. Razal, *Adv. Mater.*, 2020, **32**, e2001093.

33. T. Yun, H. Kim, A. Iqbal, Y. S. Cho, G. S. Lee, M. K. Kim, S. J. Kim, D. Kim, Y. Gogotsi, S. O. Kim and C. M. Koo, *Adv. Mater.*, 2020, **32**, 1906769.

34. Z. Ma, S. Kang, J. Ma, L. Shao, Y. Zhang, C. Liu, A. Wei, X. Xiang, L. Wei and J. Gu, *ACS Nano*, 2020, **14**, 8368-8382.

35. L. X. Liu, W. Chen, H. B. Zhang, Q. W. Wang, F. Guan and Z. Z. Yu, *Adv. Funct. Mater.*, 2019, **29**, 1905197.

36. J. Liu, H. B. Zhang, R. Sun, Y. Liu, Z. Liu, A. Zhou and Z. Z. Yu, *Adv. Mater.*, 2017, **29**, 1702367.

37. F. Shahzad, M. Alhabeb, C. B. Hatter, B. Anasori, S. M. Hong, C. M. Koo, Y.

Gogotsi, *Science*, 2016, **353**, 1137-1140.